

# Novel Volatile Barium $\beta$ -Diketone Chelates for Chemical Vapor Deposition of Barium Fluoride Thin Films

H. Sato\* and S. Sugawara

NTT Opto-electronics Laboratories, 162 Tokai, Ibaraki 319-11, Japan

Received November 4, 1992

Barium bis chelates of 1,1,1,5,5,6,6,6-octafluoro-2,4-hexanedione (Hofhd) and 1,1,1,5,5,6,6,7,7,7-decafluoro-2,4-heptanedione (Hdfhd) have been synthesized. The volatilities of these compounds were investigated by isothermal thermogravimetric analysis (ITG) and mass spectroscopy. The new chelates sublimed in a lower temperature region (190–220 °C) and exhibited better thermal stability than conventional fluorinated barium chelates, barium hexafluoroacetylacetonate [Ba(hfa)<sub>2</sub>] or barium heptafluorodimethyloctanedionate [Ba(fod)<sub>2</sub>]. They were applied to the low-pressure chemical vapor deposition (CVD) of barium fluoride (BaF<sub>2</sub>) thin films. Under an oxidizing condition, impurity-free and strongly (111)-axis-oriented BaF<sub>2</sub> films were deposited onto a silica substrate.

## Introduction

Chemical vapor deposition (CVD) techniques, including MOCVD, have been successfully applied to the growth of III–V and II–VI compound semiconductor thin films. Nowadays, CVD processes are being extended to the new fields of “oxide”<sup>1–4</sup> or “fluoride”<sup>5</sup> materials. In order to prepare films by CVD, highly volatile metal precursors with sufficient thermal stability are required for each material element. Because of this, there has been considerable interest in the development of new precursors for the CVD of fluoride and oxide films.

Of the oxide and fluoride materials, those containing Ba have several promising potential applications. These materials include barium fluoride,<sup>6</sup> zirconium fluoride–barium fluoride based fluoride glass,<sup>7,8</sup> and high-*T<sub>c</sub>* superconducting materials. Fluoride glass is the most promising candidate for ultralow-loss optical fibers.<sup>9</sup>

Several Ba  $\beta$ -diketone chelates are known as the barium precursors (Figure 1). They are barium bis chelates of tri/fluoroacetylacetonate (Htfa),<sup>5</sup> hexafluoroacetylacetonate (Hhfa),<sup>5</sup> (tri/fluoroacetyl)pivalylmethane (Htpm),<sup>10</sup> 1,1,1,2,2-(pentafluoropropanoyl)pivalylmethane (Hppm),<sup>10</sup> 2,2-dimethyl-6,6,7,7,8,8,8-heptafluoro-3,3-octanedione (Hfod)<sup>10</sup> and dipivalylmethane (Hdpm).<sup>11</sup> Ba(dpm)<sub>2</sub>, an unfluorinated compound, has been widely applied in the preparation of high-*T<sub>c</sub>* superconducting films.<sup>12,13</sup> However, these compounds have several problems, such

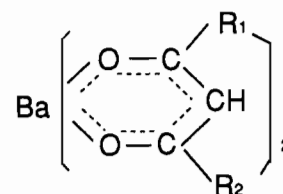


**Figure 1.** General formula of Ba  $\beta$ -diketone compounds: Ba(tfa)<sub>2</sub>, R<sub>1</sub> = CF<sub>3</sub>, R<sub>2</sub> = CH<sub>3</sub>; Ba(hfa)<sub>2</sub>, R<sub>1</sub> = R<sub>2</sub> = CF<sub>3</sub>; Ba(tpm)<sub>2</sub>, R<sub>1</sub> = CF<sub>3</sub>, R<sub>2</sub> = *t*-C<sub>4</sub>H<sub>9</sub>; Ba(ppm)<sub>2</sub>, R<sub>1</sub> = C<sub>2</sub>F<sub>5</sub>, R<sub>2</sub> = *t*-C<sub>4</sub>H<sub>9</sub>; Ba(fod)<sub>2</sub>, R<sub>1</sub> = *n*-C<sub>3</sub>F<sub>7</sub>, R<sub>2</sub> = *t*-C<sub>4</sub>H<sub>9</sub>; Ba(dpm)<sub>2</sub>, R<sub>1</sub> = R<sub>2</sub> = *t*-C<sub>4</sub>H<sub>9</sub>; Ba(ofhd)<sub>2</sub>, R<sub>1</sub> = CF<sub>3</sub>, R<sub>2</sub> = C<sub>2</sub>F<sub>5</sub>; Ba(dfhd)<sub>2</sub>, R<sub>1</sub> = CF<sub>3</sub>, R<sub>2</sub> = *n*-C<sub>3</sub>F<sub>7</sub>.

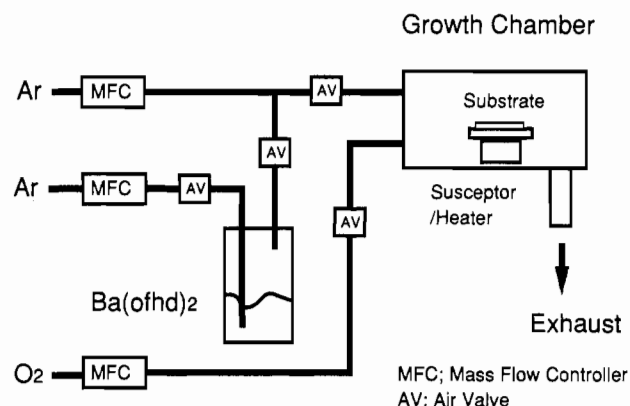


**Figure 2.** Schematic diagram of the CVD apparatus used to deposit BaF<sub>2</sub> thin film.

as a high vaporization temperature, thermal degradation during use, and variations in their vapor pressure.<sup>5,14</sup>

The difficulty in obtaining volatile barium chelates arises from the large ionic radius of barium: 1.36 Å. In order to prevent intramolecular interaction between Ba chelates or Ba atoms, we have focused on the Hofhd and Hdfhd ligands, which have a longer substituent and higher fluorination.<sup>15,16</sup>

In this paper, we report the synthesis of novel barium precursors: Ba(ofhd)<sub>2</sub> and Ba(dfhd)<sub>2</sub>. To our knowledge, alkaline earth chelates of Hofhd or Hdfhd have not yet been reported. CVD experiments were performed in order to confirm the stable gas transport of the new chelates. This paper also includes preliminary results on the preparation of barium fluoride films by CVD.

- Cowher, M. E.; Sedgwick, T. O. *J. Cryst. Growth* **1979**, *46*, 399.
- Kwak, B. S.; Zhang, K.; Boyd, E. P.; Erbil, A. *J. Appl. Phys.* **1991**, *69*, 767.
- Okada, M.; Tominaga, K.; Araki, T.; Katayama, S.; Sakashita, Y. *Jpn. J. Appl. Phys.* **1990**, *29*, 718.
- Wendel, H.; Holzschuh, H.; Suhr, H.; Erker, G.; Dehnicke, S.; Mena, M. *Mod. Phys. Lett.* **1990**, *19*, 1215.
- Purdy, P.; Berry, A. D.; Holm, R. T.; Fatemi, M.; Gaskill, D. K. *Inorg. Chem.* **1989**, *28*, 2799.
- Kirin, P. S.; Binder, R. *Nucl. Instrum. Methods Phys. Res.* **1990**, *A289*, 261.
- Fujiura, K.; Ohishi, Y.; Takahashi, S. *Jpn. J. Appl. Phys.* **1989**, *28*, L147.
- Fujiura, K.; Nishida, Y.; Kobayashi, K.; Takahashi, S. *Mater. Res. Soc. Symp. Proc.* **1992**, *244*, 121.
- Shibata, S.; Horiguchi, M.; Jinguji, K.; Mitachi, S.; Kanamori, T.; Manabe, T. *Electron. Lett.* **1981**, *17*, 775.
- Belcher, R.; Cranley, C. R.; Mayer, J. R.; Stephen, W. I.; Uden, P. C. *Anal. Chim. Acta* **1972**, *60*, 109.
- Schwarberg, J. E.; Sievers, R. E.; Moshier, R. W. *Anal. Chem.* **1970**, *42*, 1828.
- Dickinson, P. H.; Geballe, T. H.; Sanjurjo, A.; Hildenbrand, D.; Craig, G.; Zisk, M.; Collman, J.; Banning, S. A.; Sievers, R. E. *J. Appl. Phys.* **1989**, *66*, 444.
- Yamane, H.; Kurosawa, H.; Hirai, T.; Watanabe, K.; Iwasaki, H.; Kobayashi, N.; Muto, Y. *J. Cryst. Growth* **1989**, *98*, 860.

- Bade, J. P.; Baker, E. A.; Kingon, A. I.; Davis, R. F.; Bachmann, K. J. *J. Vac. Sci. Technol.* **1990**, *B8*, 327.
- Mehrotra, R. C.; Bohra, R.; Gauer, D. P. *Metal  $\beta$ -Diketonates and Allied Derivatives*; Academic Press: New York, 1978; Chapter 1, p 5.
- Richardson, M. F.; Sievers, R. E. *Inorg. Chem.* **1971**, *10*, 498.

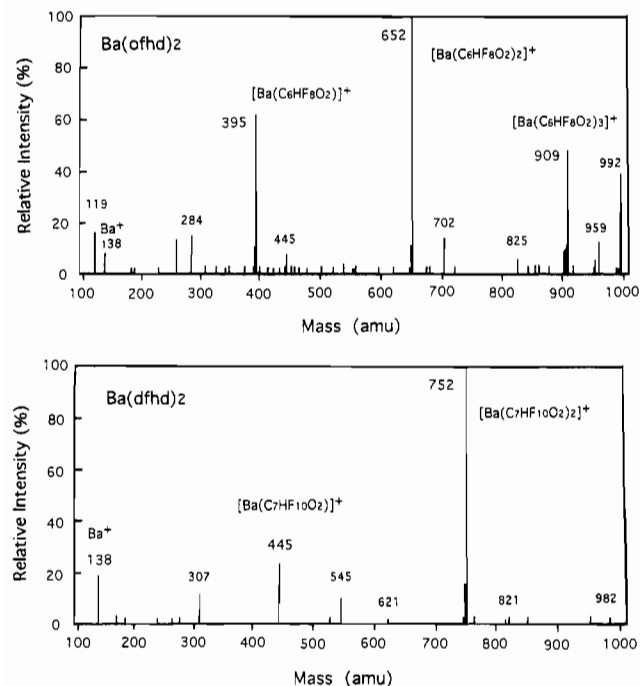


Figure 3. Mass spectra: (a, top)  $\text{Ba}(\text{ofhd})_2$ ; (b, bottom)  $\text{Ba}(\text{dfhd})_2$ .

Table I. Thermal Properties of Barium  $\beta$ -Diketone Chelates

compd	$R_1, R_2$ (Figure 1)	mp ( $^\circ\text{C}$ )	% residue <sup>c</sup>	$T'$ ( $^\circ\text{C}$ ) <sup>d</sup>
$\text{Ba}(\text{ofhd})_2$	$\text{CF}_3, \text{C}_2\text{F}_5$	233.8 <sup>a</sup>	4.0	274
$\text{Ba}(\text{dfhd})_2$	$\text{CF}_3, n\text{-C}_3\text{F}_7$	229.1 <sup>a</sup>	0.1	275
$\text{Ba}(\text{hfa})_2$	$\text{CF}_3, \text{CF}_3$	237 <sup>b</sup>	24.2	289
$\text{Ba}(\text{tpm})_2$	$\text{CF}_3, t\text{-C}_4\text{H}_9$	253 <sup>b</sup>	36.8	283
$\text{Ba}(\text{ppm})_2$	$\text{C}_2\text{F}_5, t\text{-C}_4\text{H}_9$	293 <sup>b</sup>	5.0	272
$\text{Ba}(\text{fod})_2$	$n\text{-C}_3\text{F}_7, t\text{-C}_4\text{H}_9$	191 <sup>b</sup>	9.8	291

<sup>a</sup> Determined by DSC. <sup>b</sup> Determined by DTA. <sup>c</sup> Determined by TG.

<sup>d</sup> Temperature where the baseline (100%) of the TG curve intersects the tangent of the TG curve at 50% weight.

### Experimental Section

**General Comments on Synthesis.** All manipulations were performed under an inert atmosphere (Ar or  $\text{N}_2$ ). Barium hydroxide octahydrate was obtained from Aldrich. Hofhd and Hdfhd were obtained from Fairfield. The C and H contents were determined by conventional elemental analysis. The barium content was determined by chelatometric titration.  $^1\text{H}$  and  $^{13}\text{C}$  NMR spectra were recorded on a JEOL FX100 spectrometer using acetone- $d_6$  solution.  $^{19}\text{F}$  NMR spectra were recorded on a JEOL GX270 spectrometer. The mass spectra were recorded on a VG ZAB-HF mass spectrometer: the sample was ionized by the field desorption (FD) method at 8 keV. Infrared spectra were recorded on a JEOL JIR-RFX 3002 FT-IR spectrophotometer. The melting point and heat of fusion of the samples were determined using a Mac Science DSC-3100 unit. The sublimation rate was determined under 1 Torr using a Sibata GTO-350RD glass tube oven.

**Synthesis of  $\text{Ba}(\text{dfhd})_2$ .**  $\text{Ba}(\text{OH})_2 \cdot 8\text{H}_2\text{O}$  (2.5 g) was dissolved in hot water (150  $\text{cm}^3$ ), and insoluble components ( $\text{BaCO}_3$  etc.) were filtered out. This solution was added dropwise to an Hdfhd-ethanol solution (5 g/150  $\text{cm}^3$ ) over a period of 30 min. The mixture was stirred for 24 h at room temperature in an Ar stream. Ethanol was removed in vacuo. The aqueous mixture was extracted with three 100- $\text{cm}^3$  portions of ether. The ether extracts were evaporated to dryness below 50  $^\circ\text{C}$ . The products were dried in a vacuum at 130  $^\circ\text{C}$  for 24 h, leaving a white crystalline solid. The yield was 55%.

Anal. Calcd (found) for  $\text{BaC}_{14}\text{H}_2\text{O}_4\text{F}_{20}$ : C, 22.4 (22.2); H, 0.3 (0.2); Ba, 18.3 (18.0). NMR:  $^1\text{H}$ ,  $\delta$  5.79 (CH), 2.43 (adsorbed  $\text{H}_2\text{O}$ );  $^{13}\text{C}$ ,  $\delta$  88.3 (CH), 109.6, 113.3, 124.9, 136.4 ( $\text{CF}_3$ ), 175.5 (quartet, CO);  $^{19}\text{F}$ ,  $\delta$  -0.55 (doublet,  $\text{CF}_3$ ), -4.72 (triplet,  $\text{CF}_3$ ), -43.9 (quartet,  $\text{CF}_2$ ), -50.3 (singlet,  $\text{CF}_2$ ). IR ( $\text{cm}^{-1}$ ): 3480 (m, b), 1677 (vs, sp), 1561 (vs, sp), 1510 (vs), 1369 (vs, sp), 1240 (vs), 1157 (vs), 958, 902, 799, 751, 670, 575 (s, sp). Mp: 229.1  $^\circ\text{C}$ . Heat of fusion: 9.5 kcal/mol. Sublimation rate: 39 mg/min at 220  $^\circ\text{C}$ .

**Synthesis of  $\text{Ba}(\text{ofhd})_2$ .**  $\text{Ba}(\text{ofhd})_2$  was synthesized similarly (including scale). The yield was 53%.

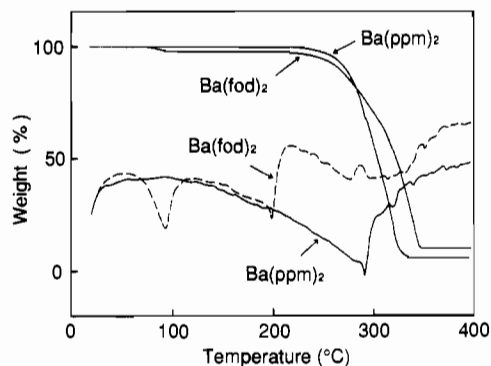
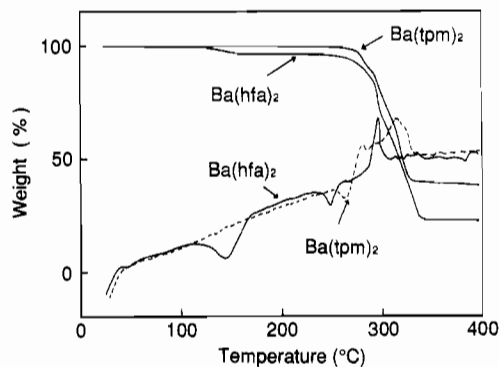
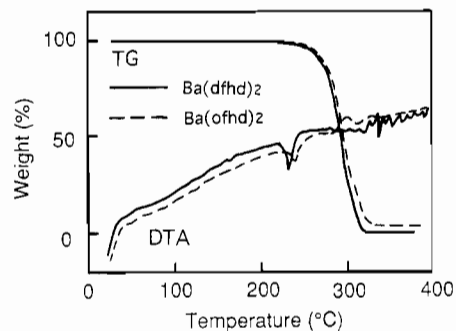


Figure 4. TG-DTA curves of Ba chelates: (a, top)  $\text{Ba}(\text{ofhd})_2$  and  $\text{Ba}(\text{dfhd})_2$ ; (b, middle)  $\text{Ba}(\text{hfa})_2$  and  $\text{Ba}(\text{tpm})_2$ ; (c, bottom)  $\text{Ba}(\text{ppm})_2$  and  $\text{Ba}(\text{fod})_2$ .

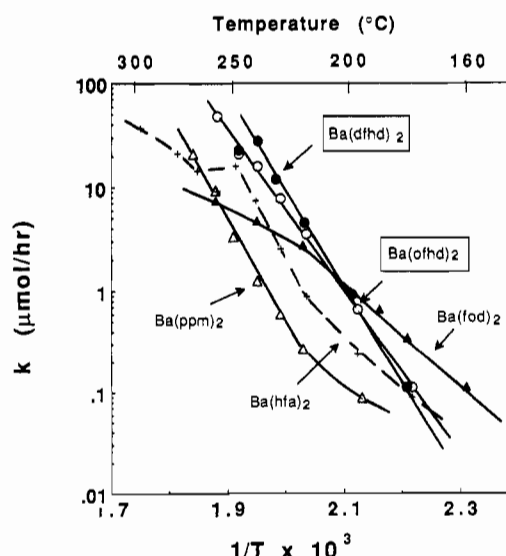


Figure 5. Arrhenius plot of  $k$  for Ba chelates.

Anal. Calcd (found) for  $\text{BaC}_{12}\text{H}_2\text{O}_4\text{F}_{16}$ : C, 21.1 (21.9); H, 0.3 (0.4); Ba, 21.1 (20.5). NMR:  $^1\text{H}$ ,  $\delta$  5.80 (CH), 2.38 (adsorbed  $\text{H}_2\text{O}$ );  $^{13}\text{C}$ ,  $\delta$  87.9 (CH), 101.7, 113.3, 124.9, 136.4 ( $\text{CF}_3$ ), 175.8 (quartet, CO);  $^{19}\text{F}$ ,  $\delta$  -0.53 (doublet,  $\text{CF}_3$ ), -6.40 (singlet,  $\text{CF}_3$ ), -46.2 (singlet,  $\text{CF}_2$ ). IR ( $\text{cm}^{-1}$ ): 3463 (s, b), 1666, 1550, 1534, 1505 (vs, sp), 1313 (m, sp), 1210,

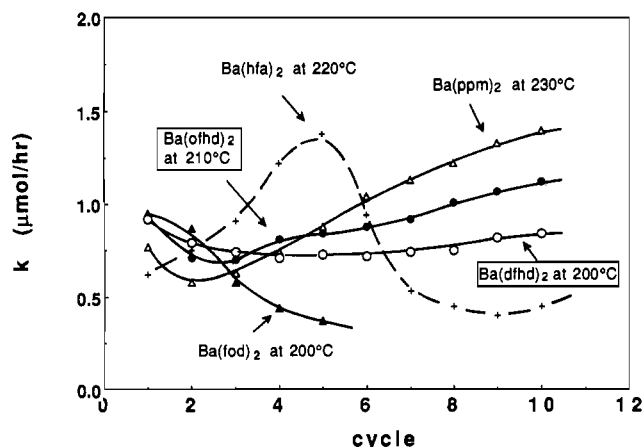


Figure 6. Heat cycle of  $k$  for Ba chelates.

1162 (vs, sp), 810, 670 (m, sp), 590 (w, sp). Mp: 233.8 °C. Heat of fusion: 5.2 kcal/mol. Sublimation rate: 3.0 mg/min at 220 °C.

**Synthesis of Conventional Ba Chelates.** Ba(hfa)<sub>2</sub>, Ba(ppm)<sub>2</sub>, and Ba(fod)<sub>2</sub> were synthesized from Ba(OH)<sub>2</sub>·8H<sub>2</sub>O and their respective ligands in aqueous ethanol.<sup>10</sup> Ba(tpm)<sub>2</sub> was synthesized from Ba metal and Htpm in ethanol.<sup>5</sup>

**Thermogravimetric Analysis.** Thermogravimetric curves were recorded with a Mac Science TG-DTA 2000 thermogravimetric analyzer in a 280 cm<sup>3</sup>/min Ar flow. The heating rate was 10 °C/min. Isothermal thermogravimetric analysis (ITG) was conducted as follows. The sample was heated at a constant temperature for between 10 and 60 min depending on the temperature, and the weight loss was recorded against time. When the weight loss arises from sublimation or vaporization, the weight decreases linearly with time and weight loss rate does not depend on the initial weight under the same boundary conditions. The determined zero-order reaction rate constant " $k$ " was adopted as the relative volatility rate. This corresponds to the tangent of the TG curve at each temperature.<sup>17</sup> Cycle ITG analysis was conducted as follows. The sample was set at the respective temperatures for 60 min and then cooled to room temperature; this cycle was repeated 10 times, and the variation in " $k$ " was evaluated.

TG-MS analysis was carried out using a TG-DTA-mass unit. The mass spectrum and TG-DTA curves were recorded simultaneously. The mass unit was a VG PC300D instrument. The capillary inlet connecting the TG unit and the mass unit was maintained at 170 °C.

**CVD Experiments.** Low-pressure CVD was performed using the apparatus shown in Figure 2. A horizontal cold-wall reactor was chosen, and Ba(ofhd)<sub>2</sub> was used as the source material. The source temperature was controlled at 210 °C and the gas line at 230 °C. Ar was used as the carrier gas at a flow rate of 550 sccm. Oxygen was introduced into the chamber through another line. The reactor pressure was 10 Torr. A silica substrate was used, and the substrate temperature was controlled at 700 °C. The film thickness was measured with a stylus profiler (Dektak 3030). The film composition was determined by X-ray fluorescence analysis. The film orientations were analyzed by X-ray diffraction. Scanning electron microscopy (SEM) was used to study the surface morphologies. Oxygen content of the film was evaluated by secondary ion mass spectroscopy (SIMS): primary ion Cs<sup>+</sup>, 14.5 kV, 5 nA; secondary ion <sup>18</sup>O<sup>-</sup>.

## Results and Discussion

**Synthesis.** Ba  $\beta$ -diketone chelates have been synthesized by several methods. BaCl<sub>2</sub>, Ba metal, and Ba(OH)<sub>2</sub> have been used as starting materials.<sup>18</sup> For Ba(ofhd)<sub>2</sub> and Ba(dfhd)<sub>2</sub>, attempts at synthesis using Ba metal or BaCl<sub>2</sub> as the starting material were unsuccessful; the products showed insufficient volatility; that is, more than 20% residue was observed after TG analysis. Furthermore, the yield was rather low when a ligand was added to the Ba(OH)<sub>2</sub> solution. Thus, Ba(OH)<sub>2</sub> was added dropwise to the solution of the ligand, instead. Details of the characteristic differences depending on the synthetic method require further

investigation. Elemental analysis and TG-DTA confirmed that Ba(ofhd)<sub>2</sub> and Ba(dfhd)<sub>2</sub> are obtained as dihydrated products before the vacuum-drying. They can be easily dehydrated under the drying conditions mentioned previously.

**Mass Spectra.** The mass spectra of Ba(ofhd)<sub>2</sub> and Ba(dfhd)<sub>2</sub> are shown in Figure 3. The molecular ion peak,  $m/e = 652$  for Ba(ofhd)<sub>2</sub> and  $m/e = 752$  for Ba(dfhd)<sub>2</sub>, can be observed in each panel as the strongest peak of the spectrum. Ba(ofhd)<sub>2</sub> shows more signals than Ba(dfhd)<sub>2</sub>. This might be ascribed to the stability difference of the chelates. When another ionization process, such as the "electron impact ionization (EI)" or "fast atom bombardment (FAB)", was used, no molecular ion signal was observed.<sup>10</sup> The chelate molecule was broken into many fragments through the strong energy of the ionization process.

**Volatilities of the Chelates.** TG-DTA curves for the Ba chelates are shown in Figure 4: (a) for the new chelates; (b, c) for the conventional chelates, Ba(hfa)<sub>2</sub>, Ba(tpm)<sub>2</sub>, Ba(ppm)<sub>2</sub>, and Ba(fod)<sub>2</sub>. The TG curves of the new chelates are quite similar. They exhibit a sharper weight loss tangent and less residue after thermogravimetric analysis than Ba(ppm)<sub>2</sub> or Ba(fod)<sub>2</sub>. The thermal properties of each chelates are listed in Table I.

TG-DTA analysis is a simple and easy way to examine the volatility of a compound. In order to obtain more practical information such as the "volatilization temperature" or the "degree of thermal decomposition", we used isothermal thermogravimetric analysis (ITG). The Arrhenius plot of " $k$ " for each chelate is shown in Figure 5. The plot shows  $\log k$  versus the inverse of absolute temperature. The linear relationship of the plots reflects the low contamination by volatile impurities or the absence of thermal decomposition. As can be seen, Ba(ofhd)<sub>2</sub> and Ba(dfhd)<sub>2</sub> have a linear dependence over a wide temperature range. Ba(hfa)<sub>2</sub> and Ba(fod)<sub>2</sub> have a poorly linear relationship. The  $k$  value of 1  $\mu\text{mol/h}$  is an empirical measure of sufficient volatility. Ba(ppm)<sub>2</sub> and Ba(hfa)<sub>2</sub> have higher volatilization temperatures than the new chelates.

Another important characteristic of CVD sources is that the compounds do not exhibit any marked thermal change during use. Such changes might be ascribed to thermal decomposition, hydrolysis,<sup>16</sup> or oligomerization.<sup>12</sup> Figure 6 shows an ITG cycle test on the chelates. With Ba(fod)<sub>2</sub>, there is a degradation in  $k$ ; Ba(hfa)<sub>2</sub> exhibits a pronounced variation in  $k$ , which increases and decreases; and with Ba(ppm)<sub>2</sub>, there is a gradual but noticeable increase in  $k$ . It seems that dehydration or a change of crystalline state might occur for Ba(ppm)<sub>2</sub>. Compared with these conventional chelates, Ba(ofhd)<sub>2</sub> and Ba(dfhd)<sub>2</sub> exhibit rather stable volatility. On the other hand, it can be seen that Ba(dfhd)<sub>2</sub> can be used at a temperature about 10 °C lower than Ba(ofhd)<sub>2</sub>.

Ba(tpm)<sub>2</sub> was also evaluated by ITG or an ITG cycle test. The results were somewhat similar to Ba(hfa)<sub>2</sub> results: poorly linear relationship in Figure 5 and pronounced variation of  $k$  in Figure 6. This compound has a very strong tendency to decompose near the sublimation point, and is not suited for CVD application.

TG-MS results for Ba(dfhd)<sub>2</sub> and Ba(fod)<sub>2</sub> are shown in Figure 7. For Ba(fod)<sub>2</sub>, at the onset of weight loss, several fragmentary signals start to increase to a considerable level; this process indicates that thermal decomposition occurs upon vaporization. Two MS signal peaks imply that two different thermal decomposition processes exist. On the other hand, very slight signal changes are observed for Ba(dfhd)<sub>2</sub>; only in the final step of the weight loss is a nonnegligible MS signal increase observed. The TG-MS results are summarized in Figure 8, which shows maximal TG weight loss versus the ratio of the maximum of carbon dioxide mass to its background (BG) level. The CO<sub>2</sub> MS signal change well relates to the TG weight loss. For conventional Ba chelates, significant decomposition occurs simultaneously with the volatilization. As can be seen, the new chelates show only slight decomposition upon vaporization.

(17) Niwkirk, A. E. *Anal. Chem.* 1960, 32, 1558.

(18) Hammond, G. S.; Nonhebel, D. C.; Wu, C. S. *Inorg. Chem.* 1963, 2, 73.

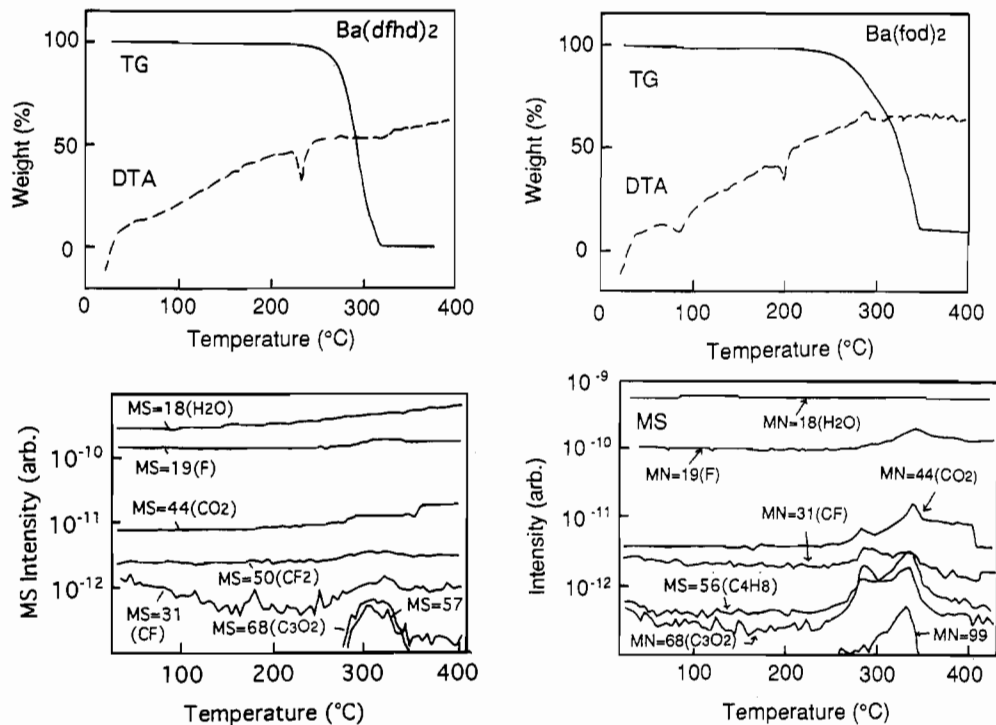


Figure 7. TG-MS analysis for  $\text{Ba}(\text{dfhd})_2$  and  $\text{Ba}(\text{fod})_2$ .

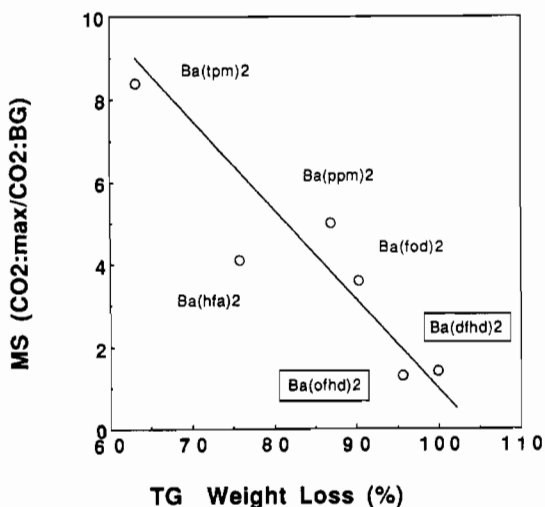


Figure 8. TG-MS results for Ba chelates.

From ITG, C-ITG, and TG-MS analysis, it can be concluded that the new chelates,  $\text{Ba}(\text{ofhd})_2$  and  $\text{Ba}(\text{dfhd})_2$ , have a lower vaporization temperature and better thermal stability than conventional Ba  $\beta$ -diketone chelates. As was mentioned in the Introduction, ofhd and dfhd ligands have a longer substituent and higher fluorination. Consequently, the ligands have a larger molar volume and could shield the Ba atom effectively. The excellent volatility, the thermal stability, and the insensitivity to hydration are all ascribed to the ofhd and dfhd ligands.

**CVD Experiments.** When only the source material was introduced into the chamber, a brown film was obtained. X-ray fluorescence analysis (XFA) showed that the film was mainly composed of stoichiometric barium fluoride, but included a large amount of carbon. Since no fluorinating agent was used, the fluorine of the barium fluoride was supplied from the source material through an intramolecular reaction. Oxygen was introduced into the chamber to reduce the carbon content of the film.<sup>5</sup>

Figure 9 shows the growth rate dependence on oxygen flow rate. As the flow rate is increased, the growth rate decreases to about half that in an oxygen-free state. The carbon signal

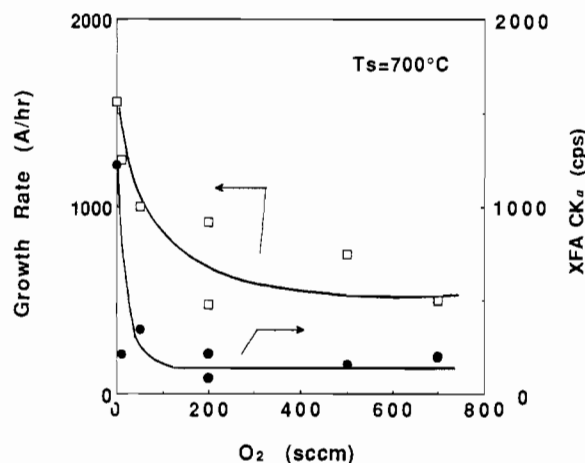


Figure 9. Growth rate dependence on oxygen flow rate.

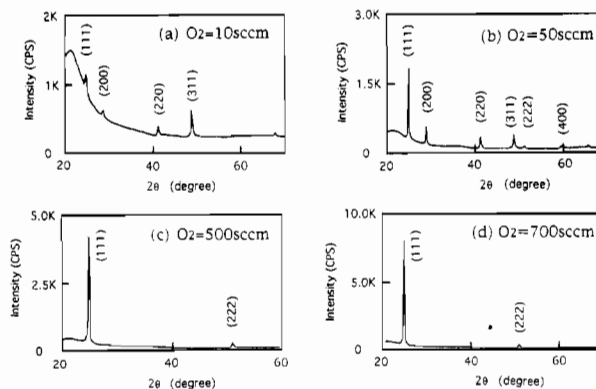


Figure 10. XRD patterns of  $\text{BaF}_2$  films prepared at different oxygen flow rates.

determined by XFA is also plotted. It is shown that even a small amount of oxygen can reduce the carbon content effectively. It is considered that the carbon is expelled mainly as carbon dioxide.

Figures 10 and 11 show X-ray diffraction patterns and SEM micrographs. At low oxygen flow rates of 10 or 50 sccm, several crystal orientation planes are observed. Cubic barium fluoride

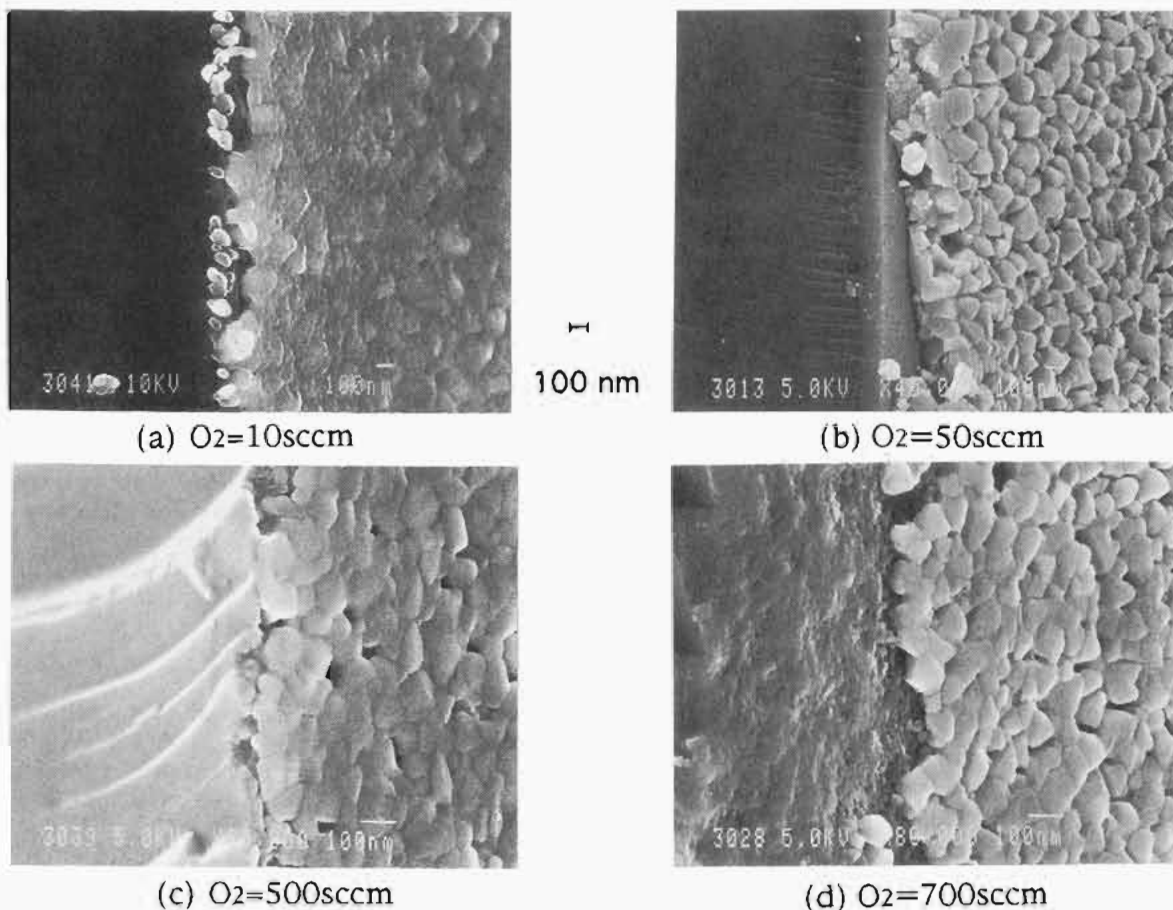


Figure 11. SEM micrographs of BaF<sub>2</sub> films prepared at different oxygen flow rates.

crystals can be seen when oxygen is introduced at a flow rate of greater than 50 sccm. As the oxygen flow rate is increased, (111)-axis orientation becomes stronger and no other plane is observed. However, it can be seen that the substrate surface has been damaged by the CVD process (700 sccm). It is assumed that the carbon is also expelled in the form of CF<sub>x</sub> or fluorine radicals; these species act as an etching gas on the quartz substrate. Barium fluoride is thermodynamically more stable than barium oxide, so barium fluoride is grown even in an oxygen atmosphere.

SIMS analysis showed that the oxygen content of the film was at the background level. It can be said that the CVD process using Ba chelate is a useful method for the preparation of high-quality barium fluoride thin films.

**Acknowledgment.** We thank Dr. K. Sugii and Dr. K. Fujiura for their encouragement and useful comments throughout the work.